9th Asia-Pacific Conference on Wind Engineering
Auckland, New Zealand
3-7 December 2017

Validating LES of the Flow in the Development Section of a Boundary Layer Wind Tunnel

J. Franke, T. H. Pham

Faculty of Engineering
Vietnamese-German University, Thu Dau Mot, Binh Duong, Vietnam

Abstract

In this study, validation results for the Large Eddy Simulation of the flow in the development section of a boundary layer wind tunnel are presented. The simulation in the empty wind tunnel with vortex generators and roughness elements is a precursor simulation to generate time–dependent inflow boundary condition for a city model investigated in the wind tunnel. Mean velocities and Reynolds stresses are compared at measurement positions located behind the roughness elements with the validation metric hit rate. For the streamwise velocity a hit rate of at least 0.634 is obtained, while the agreement for the lateral and vertical velocity components is much lower, with 0.104 and 0.000, respectively. The bad agreement is attributed to using a coarse mesh at walls without wall functions. A slightly better agreement is obtained when comparing simulation results at the location for sampling velocities within the roughness elements and the measurement locations behind the roughness elements. As the comparison of velocity spectra also indicate a good agreement at frequencies up to the cut–off frequency, it is nevertheless concluded that the sampled data can be used as inflow boundary condition for the Large Eddy Simulation of the flow in the generic city model.

Introduction

Time-dependent numerical simulation approaches like Large Eddy Simulation (LES) are increasingly used for investigating real-world problems in wind engineering. Like any other numerical simulation approach, LES must be validated for the assessment of its predictive capability. To that end experimental data should be available that allow going beyond validation with low–order statistics like mean values and variances but rather assess the full time-dependent information of simulation results. The CEDVAL–LES database [1] of the Environmental Wind Tunnel Laboratory (EWTL), Meteorological Institute, University of Hamburg, Germany, serves these needs and provides experimental time-series of velocity components and partly concentrations for different model scale complexities with the Michelstadt case being currently the most complex case. Michelstadt is a generic European city center model which was already used for validation of statistically steady Reynolds Averaged Navier Stokes (RANS) simulations [4,6] and LES [3].

A comprehensive validation of LES against the Michelstadt data is the ultimate target of the authors' research. Here results of a precursor simulation are presented and low–order statistics validated against experimental data from the CEDVAL-LES database, complexity BL3-0-0 [1]. A precursor simulation provides time-dependent inflow data on a plane for the simulation of the actual Michelstadt geometry. The simulation was performed offline so that time-series of the velocity components in the plane are first stored. A precursor simulation was preferred over a synthetic turbulence inflow boundary condition [8], trying to replicate the experimental set-up as closely as possible. The computational set-up of the simulation is explained next, before results of the simulation and its validation are shown and discussed. Conclusions are presented at the end.

Computational Parameters

Geometry, Mesh and Boundary Conditions

The computational domain has a total length of 15850 mm and width of 4000 mm, see figure 1. Its height varies between 2570 and 2622 mm in flow direction, to reduce the streamwise pressure gradient. The development section consists of six vortex generators and 35 rows of roughness elements, which are 8 more than in the authors' previous investigation [2]. Two sizes of roughness elements are used, large ones with 80 x 80 mm and small ones with 40 x 40 mm [2]. Roughness elements start at a distance of 300 mm behind the vortex generators and are always 300 mm apart in streamwise direction. Roughness elements and vortex generators are treated as zero thickness surfaces in the simulation.

The geometry of the wind tunnel, the vortex generators and roughness elements was constructed to replicate the geometry of the original wind tunnel set up. Contrary to the authors'

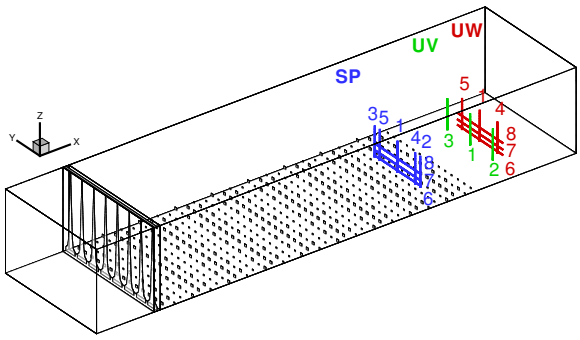

Figure 1: Computational geometry and measurement locations.

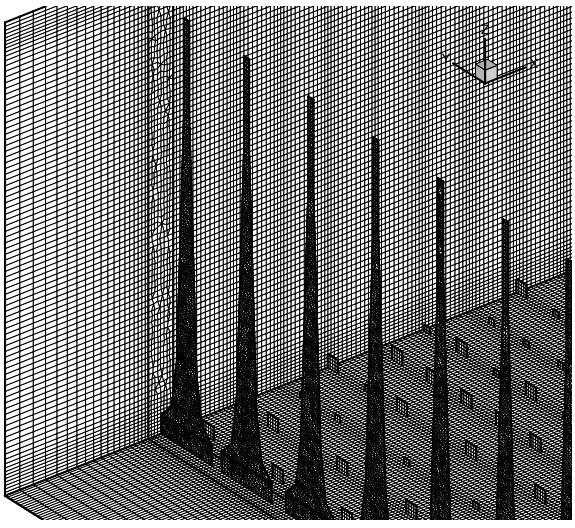

Figure 2: Surface mesh detail.

previous investigation [2] and the wind tunnel set up, the vortex generators are distributed symmetrically with respect to the wind tunnel's center plane to enable a symmetric flow field in the development section. The asymmetric placement in the wind tunnel was necessary to compensate the asymmetric approach flow, caused by the off-center placement of the wind tunnel in the laboratory.

A hybrid mesh with a total of approximately 10 million cells was created with Ansys ICEM CFD 14.5. The region around the vortex generators is meshed with an unstructured tetrahedral grid joint conformal with a hexahedral grid in the rest of the domain, see figure 2. Resolution of the roughness elements is coarse with four faces for the small and sixteen faces for the large elements. The cell height on the horizontal and lateral walls is 20 mm.

A constant velocity of 5m/s and very small subgrid scale kinetic energy are prescribed at the inflow boundary and the static pressure is fixed at the outlet, see figure 1.

Models and Numerics

Incompressible flow with constant density and viscosity was computed with OpenFOAM 2.4.0 using the `pisoFOAM` solver and the one-equation model for the subgrid scale kinetic energy to take care of the unresolved subgrid scales. The cube root of the cell volume was used as filter width. No wall function was employed despite of the coarse wall resolution.

Spatial approximations used the second-order central differencing scheme with explicit non-orthogonal correction for the diffusive terms and the second-order Gauss LUST scheme for the convective term in the momentum equation, while other equations' convective terms are approximated with the second-order central differencing scheme with gradient limiter `cellMDLimited`.

Temporal approximation was done with the implicit second-order backward differencing scheme, a convergence tolerance of 10^{-6} and a constant time-step of 0.001 s, yielding a maximum Courant number of 5 during the simulation. Statistics of the flow and pressure field in the full domain were recorded for 120 s, corresponding to approximately 48 flow through times. Time-series of velocity components were recorded at the ??? measurement locations over the same interval each 0.004 s and at the sampling plane.

Results

In contrast to the simulation data, the experimental data of CEDVAL-LES database are recorded at irregular time intervals, and over different times ranging from about 200 s to about 300 s. To match the simulation time, experimental time averages at each measurement location were first obtained for multiple intervals of 120 s lengths with consecutive intervals overlapping by 90 %. The individual time averages were then averaged to calculate the experimental mean values used for validating the simulation results. In addition, the 95 % confidence interval for these mean values was calculated.

Mean Flow Field

Experimental and numerical simulation results are compared at the measurement locations shown in figure 1 in green (UV) and red (UW) color. In addition, simulation results at corresponding locations within the sampling plane (SP, blue) are compared to the measurements at UV and UW profiles. Measurements were done with a 2D Laser Doppler Anemometer (LDA), yielding only the two named mean velocity components and corresponding Reynolds stresses at the measurement locations. All mean velocities and Reynolds stresses are made non-dimensional with the mean streamwise velocity component at $z = 444$ mm height of the profile UV1, cf. figure 1.

Figure 3 shows the mean streamwise velocity $\langle U \rangle / U_{ref}$ at the central profiles SP1 (blue), UV1 (green) and UW1 (red). Error bars for the experimental data represent the 95 % confidence intervals from averaging the individual 120 s time averages.

From approximately $z = 0.3$ m the agreement between simulation and experiment is very good. Below this height, the simulation yields too high streamwise velocities close to the ground due to the coarse grid at the wall and the omission of wall functions. Therefore the simulated wall shear stress is too small to generate a momentum reduction as observed in the experiments.

The simulated streamwise velocity within the roughness elements (blue) agrees however very well with experiments all the way down to the lowest measurement position. There the form drag of the roughness elements provides appropriate momentum reduction, even with the coarse mesh resolution.

The mean lateral and vertical velocity components at the central profiles have a much smaller magnitude than the streamwise component, which has to be taken into account when looking at figure 4 and 5 where they are displayed. The simulated mean lateral velocity component is closer to zero than the experiment, which is to be expected from the purely symmetric geometry of the computational domain. Differences between simulation and experiment are small, but mostly larger than the experimental 95 % confidence intervals.

Contrary to this, the differences between the simulated and measured vertical velocity component at the central location is more pronounced. The experimentally observed downward flow at UW1 is more profound over the entire height of the measurements, with the simulation in some regions even displaying a slight upward movement.

Quantitative comparison of simulated and experimental mean velocities is done with the validation metric hit rate [7]. The allowed relative difference between simulation and experiment is 0.25 and for the allowed absolute difference the local 95 % confidence interval of the experiments is used. Hit rates have been determined for all UV and UW measurement points, as well as for the comparison of the simulation data at the sampling plane and the corresponding UV and UW positions. The results are shown in table 1.

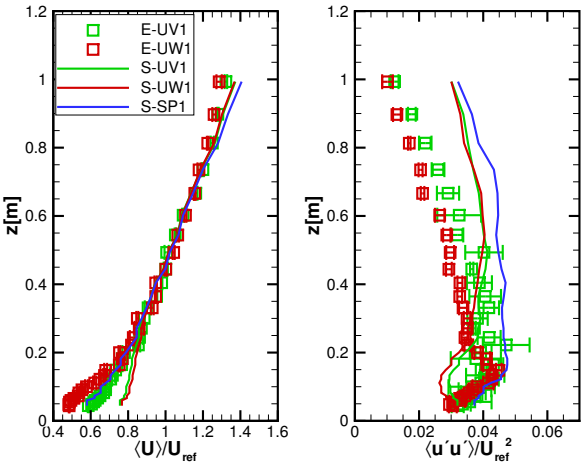

Figure 3: $\langle U \rangle / U_{ref}$ and $\langle u'u' \rangle / U_{ref}^2$ at $y = 0$ m. For locations see figure 1.

Location	$\langle U\rangle/U_{ref}$	$\langle V\rangle/U_{ref}$	$\langle W\rangle/U_{ref}$	$\langle u'u'\rangle/U^2_{ref}$	$\langle v'v'\rangle/U^2_{ref}$	$\langle w'w'\rangle/U^2_{ref}$	$\langle u'v'\rangle/U^2_{ref}$	$\langle u'w'\rangle/U^2_{ref}$
SP-UV	1.000	0.115	–	0.750	0.354	–	0.417	–
SP-UW	1.000	–	0.078	0.601	–	0.340	–	0.307
UV	0.792	0.104	–	0.698	0.615	–	0.313	–
UW	0.634	–	0.000	0.673	–	0.536	–	0.294

Table 1: Hit rates of mean velocities and Reynolds stresses.

As anticipated from the graphical presentation, streamwise velocities from the sampling plane agree very well with the experiments at UV and UW locations, while the agreement for the velocity with small magnitude is much worse, leading even to a hit rate of 0.000 for the mean vertical velocity component at UW locations.

A similar behavior is observed for the hit rates of the Reynolds stress components, although there the agreement is in two cases better at the measurement locations themselves. The straemwise and lateral normal Reynolds stresses agree very well with the experiments also close to the wall. At larger heights the simulation consistently predicts larger normal Reynolds stresses than the experiment, which could be due to insufficient resolution of smaller structures that could break up large structures with high energy [5].

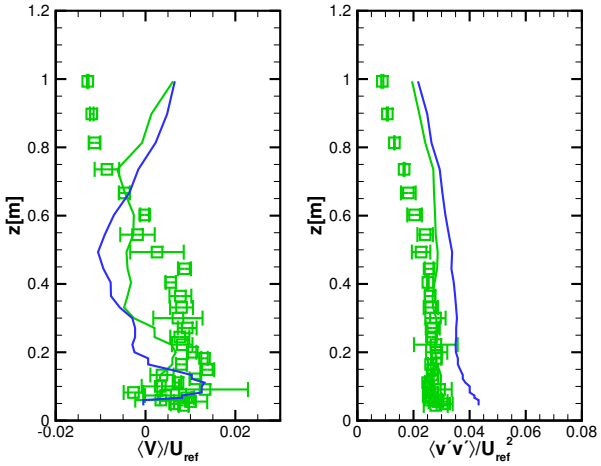

Figure 4: $\langle V\rangle/U_{ref}$ and $\langle v'v'\rangle/U^2_{ref}$ at $y = 0$ m. For definitions see figure 3.

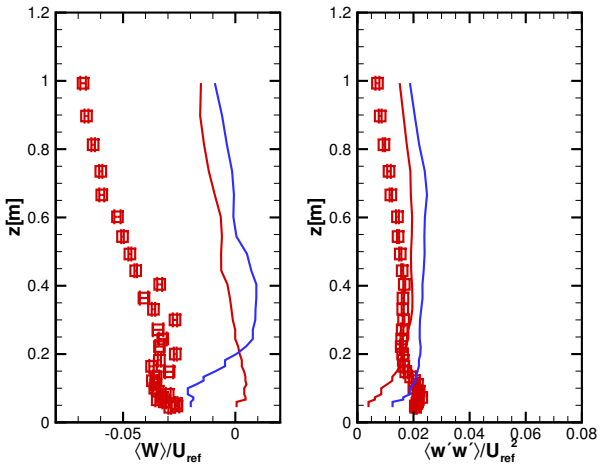

Figure 5: $\langle W\rangle/U_{ref}$ and $\langle w'w'\rangle/U^2_{ref}$ at $y = 0$ m. For definitions see figure 3.

Finally it is noted that the simulation and the experiment display a constant flux layer with approximately the same extent, see $\langle u'w'\rangle/U^2_{ref}$ in Figure 6. The simulation does however predict a much larger magnitude of the vertical Reynolds shear stress, especially within the roughness elements. There the fluctuations generated by the roughness elements are much higher than the ones generated in the underresolved wall adjacent flow behind the roughness elements.

Spectra

Experimental and simulation velocity spectra have been compared at all measurement locations. Power Spectral Densities (PSDs) were computed using a Hamming window of 10 s with 50 % overlap. The unevenly sampled experimental time–series were made evenly sampled using interpolation with splines of third order.

Velocity spectra of the streamwise velocity are shown on figure 7 and 8 for two different heights at measurement location UV1. PSDs S_{uu} are made non–dimensional with the variance σ^2_u, and the frequency f is non–dimensionalized with the local height z and mean streamwise velocity component $\langle U\rangle$. Experimental spectra are obtained and plotted for each of the 120 s segments of the entire time–series, and three theoretical spectra have also been included.

For low frequencies the simulation results agree well with the measured and the theoretical spectra. The cut–off frequency is however reached relatively fast, due to the relatively large spatial filter width induced by the coarse mesh. Very well visible is the lower cut–off frequency at the first location off the bottom wall, figure 7, as compared to the cut–off frequency at the position furthest from the bottom wall, figure 8.

The resolution of the simulation is estimated by comparing the areas under the spectral curves. Like in the previous investigation [2], the present LES resolves 65–80 % of the energy,

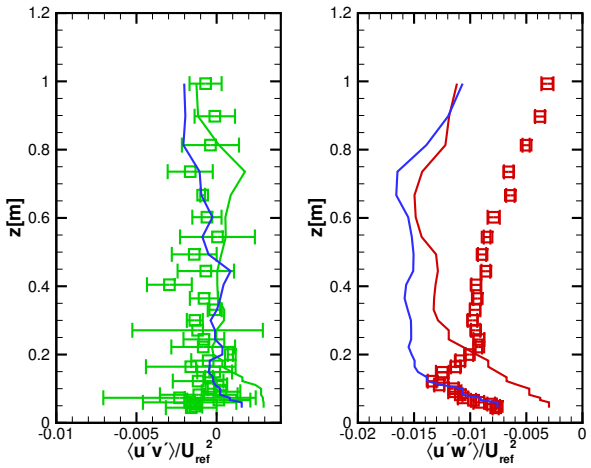

Figure 6: $\langle u'v'\rangle/U^2_{ref}$ and $\langle u'w'\rangle/U^2_{ref}$ at $y = 0$ m. For definitions see figure 3.

representative of a Very Large Eddy Simulation (VLES).

Conclusions

LES of the flow in the development section of a boundary layer wind tunnel has been performed as a precursor simulation to sample time–dependent velocities on a plane that shall in the future be used as inflow data for the LES of the flow over a generic city center model.

- The coarse grid at the walls together with the omission of wall functions leads to insufficient wall shear stress and therefore too high streamwise velocities close to the bottom wall.
- Simulation results at the sampling plane within the roughness elements agree much better with experiments close to the wall.
- Hit rates for the streamwise velocity normal Reynolds stress are high, while the other hit rates are low, partly also due to the very small allowed absolute differences resulting from the experimental 95 % confidence intervals.
- Velocity spectra show that the LES resolves 65–80 % of the energy measured in the wind tunnel, so that the simulation should be rather referred to as Very Large Eddy Simulation (VLES).
- Despite the shortcomings presented above, the sampled data are considered as sufficiently accurate to be used as inflow condition for the validation of LES for the Michelstadt case.

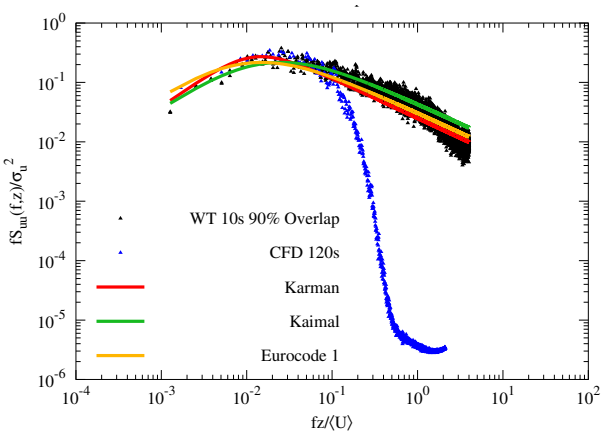

Figure 7: Streamwise velocity spectra at UV1, $z = 0.04889$ m.

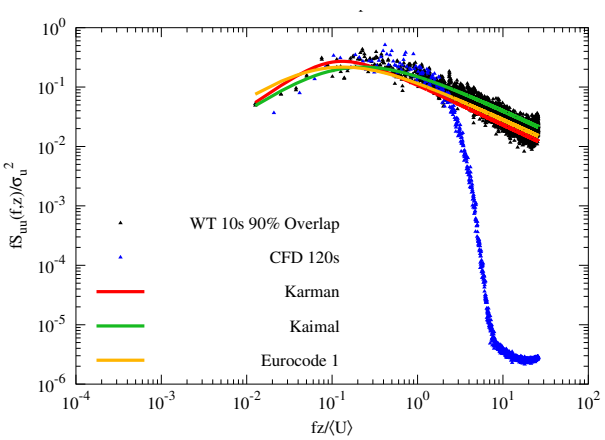

Figure 8: Streamwise velocity spectra at UV1, $z = 0.99333$ m.

Acknowledgements

Computing time for the simulation has been generously provided on the High Performance Computing cluster of the Faculty of Computer Science & Engineering, Ho Chi Minh University of Technology, Ho Chi Minh City, Vietnam.

References

[1] Fischer, R., Bastigkeit, I., Leitl, B. and Schatzmann, M., Generation of spatio-temporally high resolved datasets for the validation of LES-models simulating flow and dispersion phenomena within the lower atmospheric boundary layer, in *5th International Symposium on Computational Wind Engineering: CWE2010*, Chapel Hill, North Carolina, USA, 2010.

[2] Franke, J. and Pham, T.H., Precursor Simulation for LES Validation Study of the Michelstadt Case, in *7th European–African Conference on Wind Engineering: EACWE2017*, Liege, Belgium, 2017.

[3] Gariazzo, C., Leitl, B., Castelli, S.T., Baumann–Stanzer, K., Reisin, T.G., Barmpas, F., Tinarelli, G., Milliez, C.M., Bemporad, E. and Armand, P., COST Action ES1006. Evaluation, Improvement and Guidance of Local-Scale Emergency Prediction and Response Tools for Airborne Hazards in Built Environments: Ongoing Activities, Experiments and Recent Results, *Chemical Engineering Transactions*, **36**, 2014, 529–534.

[4] Hertwig, D., Efthimiou, G.C., Bartzis, J.G. and Leitl, B., CFD-RANS model validation of turbulent flow in a semi-idealized urban canopy, *J. Wind Eng. Ind. Aerodyn.*, **111**, 2012, 61–72.

[5] Manickam, B., Franke, J., Muppala, S.P.R. and Dinkelacker, F., Large-eddy Simulation of Triangular-stabilized Lean Premixed Turbulent Flames: Quality and Error Assessment, *Flow Turbulence Combustion*, **88**, 2012, 563–596.

[6] Rakai, A. and Franke, J., Validation of two RANS solvers with flow data of the flat roof Michelstadt case, *Urban Climate*, **10**, 2014, 758–768.

[7] Schatzmann, M., Olesen, H. and Franke, J., *COST 732 Model Evaluation Case Studies: Approach and Results*, COST Office, 2010.

[8] Tabor, G.R. and Baba-Ahmadi, M.H., Inlet conditions for large eddy simulation: A review, *Computers & Fluids*, **39**, 2010, 553–567.